Improved high-resolution magnetic resonance imaging using a cylindrical k-space sampling method

R. Chamberlain[1], T. M. Wengenack[2], J. F. Poduslo[2], C. R. Jack[3], and M. Garwood[1]

[1]Center for Magnetic Resonance Research, University of Minnesota, Minneapolis, MN, United States, [2]Departments of Neurology, Neuroscience, and Biochemistry/Molecular Biology, Mayo Clinic College of Medicine, Rochester, MN, United States, [3]Department of Radiology, Mayo Clinic College of Medicine, Rochester, MN, United States

Introduction

MRI has proven to be a useful modality for visualizing amyloid plaques in transgenic mouse models of Alzheimer's disease. Plaques provide a unique and difficult imaging target because they can be on the order of one voxel in size, and the images typically have low SNR due to the high resolution needed. Traditional MRI acquires data on a Cartesian grid, with the total extent of sampling bounded by a rectangular box. The point-spread function (PSF) and SNR of the final image can be improved using a different method of k-space sampling[1]. This work compares the PSF and contrast-to-noise ratio (CNR) of the plaques in images among a rectangular k-space sampling method and three different cylindrical methods.

Methods

Ex vivo imaging was performed on the brain of a 9-month-old doubly transgenic (APP/PS1) mouse that had been fixed and embedded in agar gel. Images were acquired at 9.4 T with a 3D spin echo sequence[2]. Four different k-space acquisition schemes, shown in Fig. 1, were used. In all cases the readout direction, *x*, was acquired with 256 points and the 3D matrix was zero-filled to 512 x 192 x 128 points, giving an apparent isotropic resolution of 30 μm. Although the voxel size was directionally symmetric, the FOV was directionally asymmetric in order to optimally accommodate the anatomy of the mouse brain. The rectangular k-space sampling gave a nominal resolution of 60 μm (prior to zero-filling) in all three directions, and was used as the standard technique, case 1. Case 2 (outermost circle) took the same total scan time as case 1, but was designed to give a resolution that was rotationally invariant. Case 3 (middle circle) reduced the total scan time by 22% while giving a rotationally invariant PSF with the same nominal resolution as case 1. Case 4 acquired the middle circle and used the extra scan time to acquire the ring between the middle and innermost circles a second time. This reduced the noise in the highest spatial frequency region, with a scan time equal to case 1. The techniques were compared by manually identifying 680 plaques in the 3D volume and then calculating CNR of each identified plaque in all four cases.

Results and Discussion

The PSFs of the four cases are shown in Fig. 2. The PSFs of the circular cases are rotationally invariant, while the PSF of the rectangular case is not. The PSFs indicate that there will be a loss in effective resolution for cases 3 and 4 for all orientations. Case 2 will have a resolution gain in the *y* and *z* directions and a resolution loss in the diagonal directions. However, the resolution changes are very slight and have minimal impact on the images. Figure 3 shows the same magnified region for all four cases. The average CNR across all 680 identified plaques are given above the image. For the same scan time as the traditional rectangular sampling (case 1), the circular technique with averaging of the edges (case 4) can increase plaque CNR by 22%. Sampling the inscribed circle, case 3, can increase plaque CNR by 16% with a 22% reduction in scan time. These results indicate that the rectangular sampling scheme is not optimal. It is postulated that this is because plaques are approximately spherically symmetric, so they deposit energy in k-space in a spherically symmetric manner; therefore, the most efficient sampling of that energy should also be spherically symmetric. With the practical constraints of a Cartesian pulse sequence, a cylindrical sampling scheme is the most logical choice.

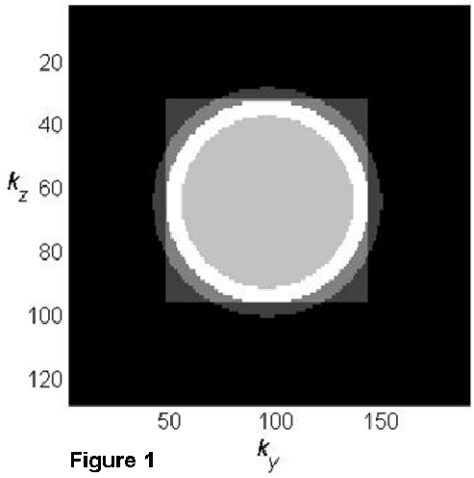

Figure 1

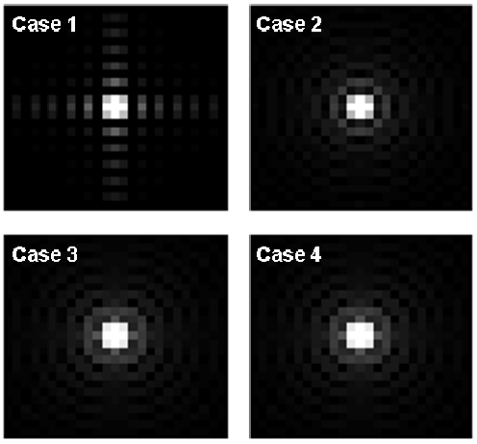

Figure 2

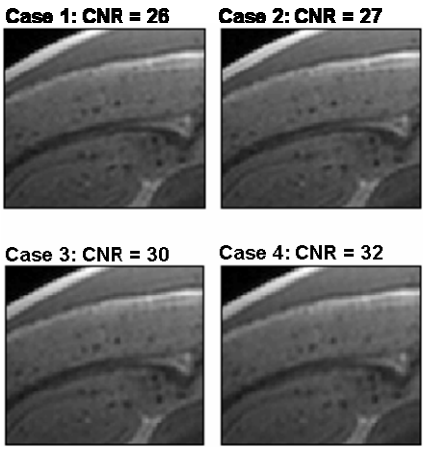

Figure 3

References

[1] Bernstein MA, *et al*, *JMRI* **14**: 270 (2001). [2] Jack CR, *et al*, *MRM* **52**: 1263 (2004).

Acknowledgements

Supported by NIH P41 RR008079 and P30 NS057091, the Keck Foundation, and the MN Partnership for Biotech and Med Genomics.